



Synthesis and Structural Insights of Transition Metal Complexes Assembled by 1,4-Cyclohexanedicarboxylic Acid and 1,10-Phenanthroline

S. Shanjitha^{a,*}

^a Department of Chemistry, Kangeyam Institute of Technology, Tamil Nadu-638108, India

* Corresponding author Email: shanjithachem@gmail.com

DOI: <https://doi.org/10.54392/nnxt2512>

Received: 06-01-2025; Revised: 12-03-2025; Accepted: 18-03-2025; Published: 25-03-2025

Abstract: In this study, a series of transition metal complexes involving Zn(II), Cd(II) and Ni(II) were synthesized using 1,4 - Cyclohexane dicarboxylic acid (CHDA) and 1,10 - Phenanthroline (Phen) as co-ligands. These bidentate and flexible ligands were selected for their ability to form stable and multifunctional coordination frameworks. Comprehensive characterization was performed using FT-IR, PXRD, TGA, SEM, and EDAX techniques to evaluate the structural, thermal, and morphological attributes of the complexes. FT-IR confirmed coordination via carboxylate oxygen and nitrogen atoms, while PXRD revealed varying degrees of crystallinity influenced by metal-ligand interactions. TGA demonstrated distinct thermal decomposition profiles, indicating the formation of thermally stable metal oxides. SEM analysis showed metal-specific morphologies, ranging from amorphous to crystalline textures. The results underscore the potential of these complexes in applications such as catalysis, sensing, and materials engineering, where thermal stability and structural tunability are critical.

Keywords: 1,4-Cyclohexanedicarboxylic acid, 1,10-Phenanthroline, Metal complexes, Thermal stability, Transition metal

1. Introduction

Transition metal complexes have been extensively studied due to their intriguing structural diversity and wide range of applications in catalysis, sensing, and optoelectronic materials. The choice of ligands plays a crucial role in dictating the physicochemical properties and stability of such complexes. Among the various ligands, 1,4-Cyclohexane dicarboxylic acid (CHDA) and 1,10-Phenanthroline (Phen) have emerged as versatile chelating agents capable of forming robust metal-organic frameworks and coordination complexes with interesting electronic and thermal properties [1, 2]. Carboxylate ligands such as CHDA have been widely explored for their ability to form coordination networks with transition metals, offering structural rigidity and enhanced thermal stability [3-5]. Studies have demonstrated that CHDA, due to its flexible aliphatic backbone, allows for diverse coordination modes, leading to the formation of supramolecular architectures with tunable porosity and stability [6-8]. In particular, zinc and cadmium complexes with dicarboxylate ligands have exhibited promising applications in gas adsorption and catalysis. On the

other hand, Phen is a well-known bidentate ligand that imparts additional electronic and photophysical properties to metal complexes. Its conjugated planar structure enhances metal-ligand interactions, making Phen-based complexes valuable in redox catalysis, luminescent materials, and molecular sensing [9, 10]. Ni(II), Ru(III), and other transition metals coordinated with Phen have been studied for their potential in electrochemical and photocatalytic applications, owing to their stability and ability to mediate electron transfer reactions [4, 11-14]. Despite these advancements, there is still limited research on the combined influence of CHDA and Phen ligands in metal complexes and their structural characterization. In this study, we report the synthesis and comprehensive characterization of Zn(II), Cd(II) and Ni(II) complexes incorporating CHDA and Phen ligands. The complexes were synthesised systematically and by correlating the structural characteristics with thermal and morphological properties, we aim to establish their potential applications in catalysis, gas sensing, and electronic materials. The findings from this study contribute to the growing body of knowledge on multifunctional metal-organic complexes, providing

insights into their structure-property relationships and practical usability in advanced material applications.

2. Experimental Methods

2.1 Materials and Methods

All the reagents and solvents utilized for the synthesized were purchased from Sigma Aldrich, India.

2.2 Characterisation Techniques

FT-IR spectrum of the complex were recorded using Shimadzu (IR Affinity 1) and UV-250 spectrometer between the range of 400 and 4500 cm^{-1} . The phase characterisation of the prepared metal complex samples were carried out using powder X-ray diffraction unit (M/s Explorer GNR, Italy) with $\text{Cu K}\alpha$ radiation ($\lambda = 1.5418 \text{ \AA}$) and Ni filter. The diffraction patterns were recorded from $20^\circ - 60^\circ$ in steps of 0.02° with an integration time of 1 s at each step. The thermal stability and different stages of decomposition

of the complex was studied from 25 to 600 $^\circ\text{C}$ using SHIMADZU DTG-60. Further, the morphology elemental composition of the complex were confirmed using the results from FEI Quanta FEG 200 model - Scanning Electron Microscope, accompanied with EDAX.

2.3 Synthesis of NCP

A mixture of $\text{NiCl}_2 \cdot 6\text{H}_2\text{O}$, 1,10-Phenanthroline, 1,4-Cyclohexane dicarboxylic acid in the molar ratio of 2:1:2 in ethanol was refluxed at 80°C for 2h. The resulting green coloured precipitate was filtered and washed with ethanol. The reaction scheme is shown in figure 1.

2.4 Synthesis of ZCP

A mixture of $\text{ZnCl}_2 \cdot 6\text{H}_2\text{O}$, 1,10-Phenanthroline, 1,4-Cyclohexane dicarboxylic acid in the molar ratio of 2:1:2 in ethanol was refluxed at 80°C for 5h. The white precipitate was filtered and washed with ethanol. The synthesis of ZCP is depicted in figure 2.

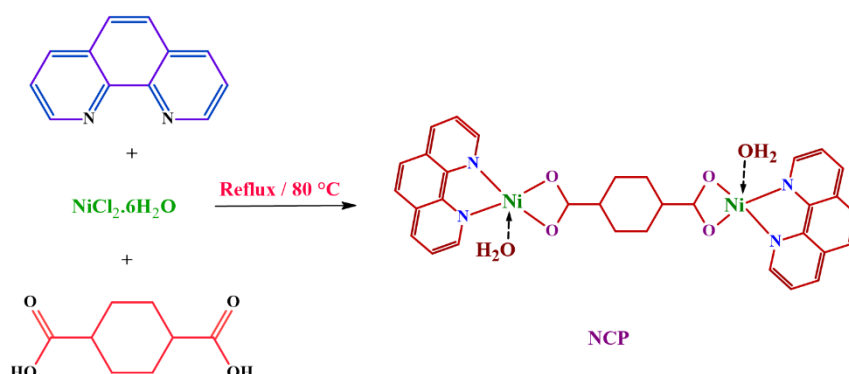


Figure 1. Reaction scheme for the synthesis of NCP

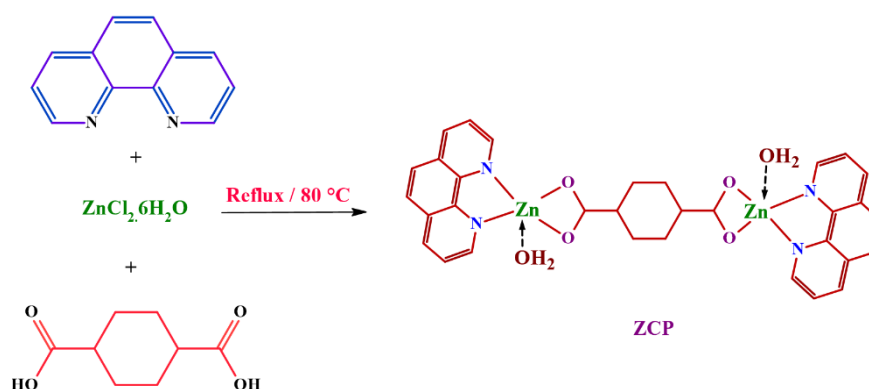


Figure 2. Reaction scheme for the synthesis of ZCP

2.5. Synthesis of DCP

A mixture of $\text{Cd}(\text{CH}_3\text{COO})_2 \cdot 2\text{H}_2\text{O}$, 1,10-Phenanthroline, 1,4-Cyclohexane dicarboxylic acid in the molar ratio of 2:1:2 in ethanol was refluxed at 80 °C for 4h. The resulting white precipitate was filtered and washed with ethanol. The scheme involved in synthesis of DCP is shown in figure 3.

3. Results and Discussion

3.1. FT-IR Spectroscopy

The stacked FT-IR spectrum of the complexes are shown in figure 4. The free CHDA exhibits a strong and broad stretching band in the range of 1700–1720 cm^{-1} , which is attributed to the C=O stretching of the carboxyl group. In the metal complexes, this band shifts to a lower frequency (1550–1650 cm^{-1}) due to the chelation of the carboxylate group with the metal center, confirming coordination. The asymmetric ($\nu_{\text{as}} \text{COO}^-$) and symmetric ($\nu_{\text{s}} \text{COO}^-$) stretching frequencies of coordinated carboxylates appear between 1550–1600 cm^{-1} and 1350–1450 cm^{-1} respectively. The $\Delta\nu < 200 \text{ cm}^{-1}$, suggests bidentate coordination of ligand with the metal center [15, 16]. The sp^3 C-H stretching vibrations of the cyclohexane ring are observed in the range of 2800–3000 cm^{-1} , indicating the presence of the aliphatic backbone. The C-H bending appears in the region of 1300–1450 cm^{-1} . The characteristic C=N stretching of the heterocyclic ring in Phen appears in the region of 1580–1620 cm^{-1} . A noticeable shift in this band upon complexation confirms the coordination of nitrogen atoms with the metal center. The M-O stretching vibrations appear in the 400–600 cm^{-1} region, confirming the binding of

carboxylate groups to the metal ions. The M-N stretching frequencies, indicative of coordination through nitrogen donor atoms, appear in the 450–550 cm^{-1} region [17, 18].

3.2 Powder X-Ray Diffraction

PXRD analysis is a crucial technique for determining the crystallinity, phase purity, and structural characteristics of metal complexes. The PXRD pattern (figure 5) of DCP shows weak peaks, indicating a non-crystalline nature. The presence of multiple high-intensity reflections between 5° and 40° (2θ) suggests a partially ordered arrangement of the molecules in a structured lattice. The sharp peaks at low 2θ values could be due to strong intermolecular interactions and periodic ordering within the unit cell.

The PXRD pattern of NCP shows multiple peaks, though with slightly broader reflections compared to DCP. The moderate sharpness of the peaks suggests a semi-crystalline nature, meaning it has both amorphous and crystalline regions. The broader peaks may be attributed to microstructural effects such as small crystallite size or lattice strain. The PXRD pattern of ZCP shows weak and broad peaks, indicating a low degree of crystallinity or possible amorphous nature. The lack of sharp reflections suggests disorder in the packing of the complex, which may be due to coordination flexibility or weak intermolecular interactions. The broad hump around 10°–30° (2θ) is characteristic of materials with significant amorphous character, possibly due to solvent effects or polymeric interactions in the solid state [17, 19-21].

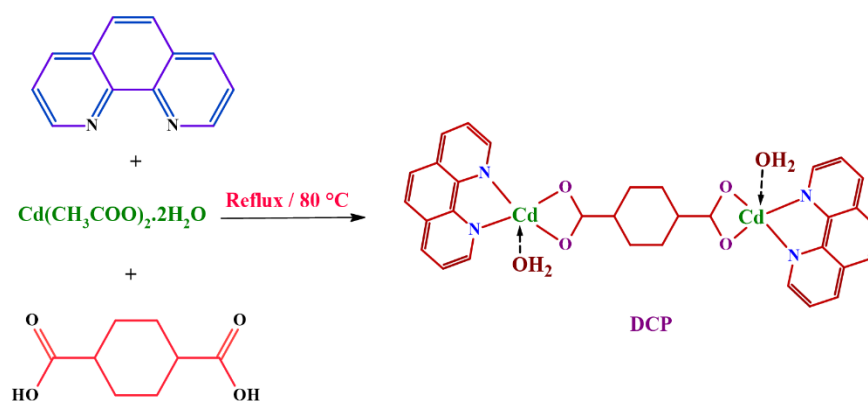


Figure 3. Reaction scheme for the synthesis of DCP

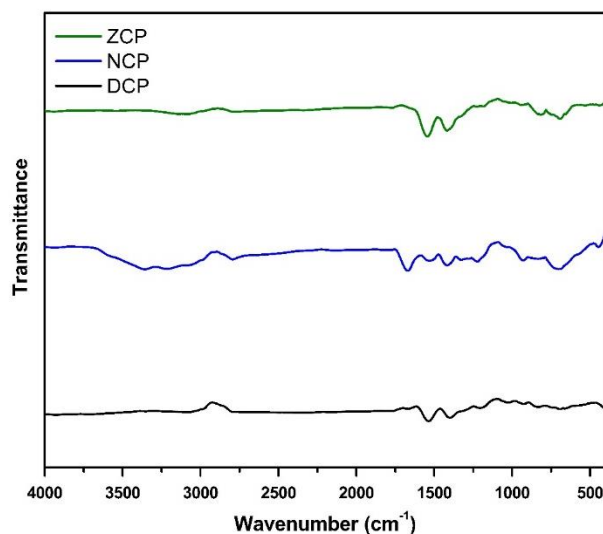


Figure 4. FT-IR spectrum of the synthesized complexes

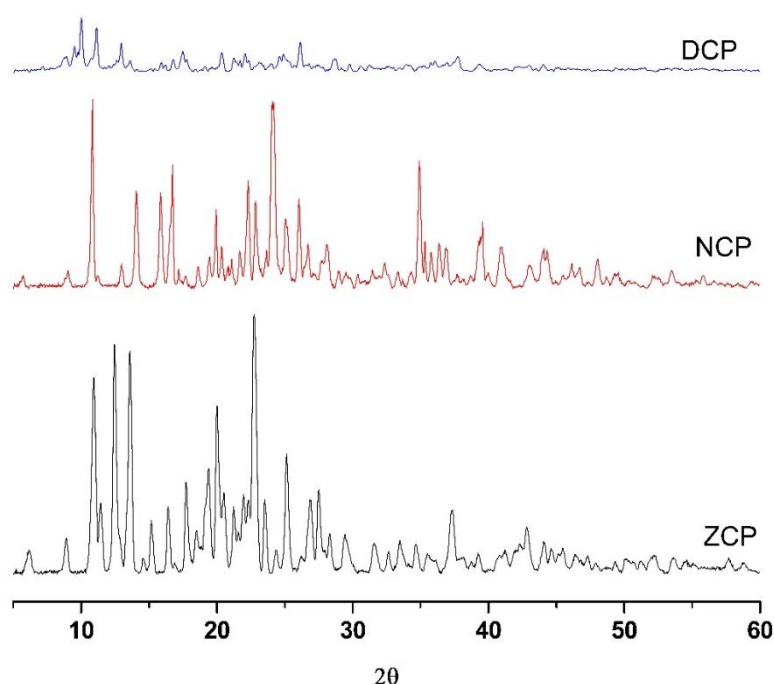


Figure 5. PXRD pattern of the synthesized complexes

3.3 Thermogravimetric Analysis

The TGA curve provides insight into the thermal stability and decomposition pathway of the coordination complex. The Ni-based coordination complex exhibits thermal stability up to $\sim 250^{\circ}\text{C}$. The major decomposition occurs in two steps where the first stage of decomposition ($\sim 28.2\%$, below 300°C) corresponds to the removal of solvent molecules (fig 6). The temperature range suggests the loss of physically adsorbed or weakly coordinated water molecules. The second stage of decomposition

($\sim 34.4\%$, $300\text{--}600^{\circ}\text{C}$) is likely due to the decomposition of the organic ligands (CHDA and Phen). The complete thermal decomposition thus corresponds to the complete degradation of the organic framework, leaving behind the residual metal oxide (NiO). The TGA curve of the zinc complex (fig 7) containing 1,4-cyclohexane dicarboxylic acid and 1,10-phenanthroline shows first weight loss ($\sim 18.1\%$) at lower temperatures ($\sim 200\text{--}300^{\circ}\text{C}$) corresponding to the removal of lattice or coordinated water molecules. The second weight loss ($\sim 35.0\%$) in the range of

~300-600°C suggests the decomposition of organic ligands (1, 4-cyclohexane dicarboxylic acid and 1, 10-phenanthroline). The presence of phenanthroline may contribute to a significant mass loss due to its aromatic structure. The total decomposition results in the formation of likely zinc oxide (ZnO). The TGA curve of DSP (figure 8) reveals two different stages of decomposition where the first stage (~21.9%, Below 300°C) corresponds to the loss of solvent molecules (such as coordinated water or lattice solvents). The temperature range indicates the removal of physically adsorbed or weakly coordinated molecules. The second weight loss (~41.9%, 300–600°C) is associated with the decomposition of the organic ligands (cyclohexane dicarboxylic acid and phenanthroline). The breakdown of the carboxylate groups and aromatic rings occurs in this region, contributing to significant weight reduction.

The total weight loss (~75.9%) represents the complete degradation of the organic framework, leaving behind a stable inorganic residue. The remaining weight suggests the formation of Cadmium-based metal oxide [19, 22, 23].

3.4. Scanning Electron Microscopy (SEM)

The surface morphology of the synthesized metal complexes was investigated using scanning electron microscopy (SEM) and are depicted in figure 9-11. The Ni, Cd, and Zn complexes exhibited distinct morphological characteristics, highlighting the influence of metal coordination on the crystal growth and surface structure. The SEM images of the nickel complex revealed indefinite morphology with a rough surface.

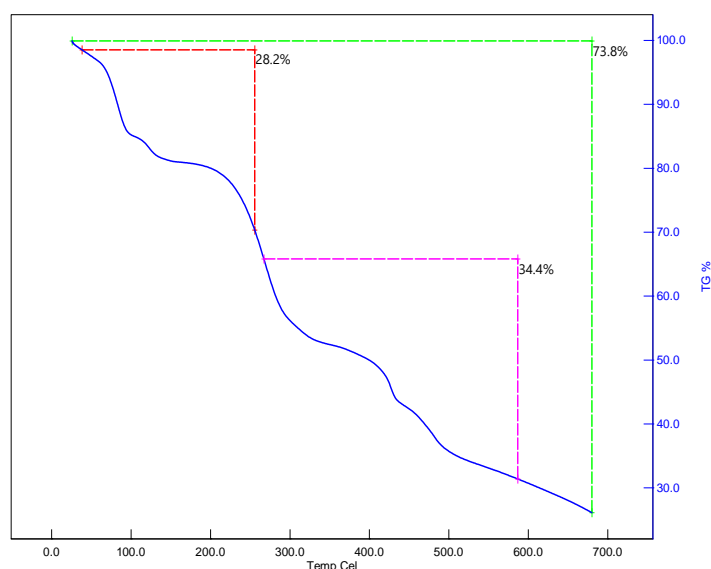


Figure 6. TGA graph of NCP

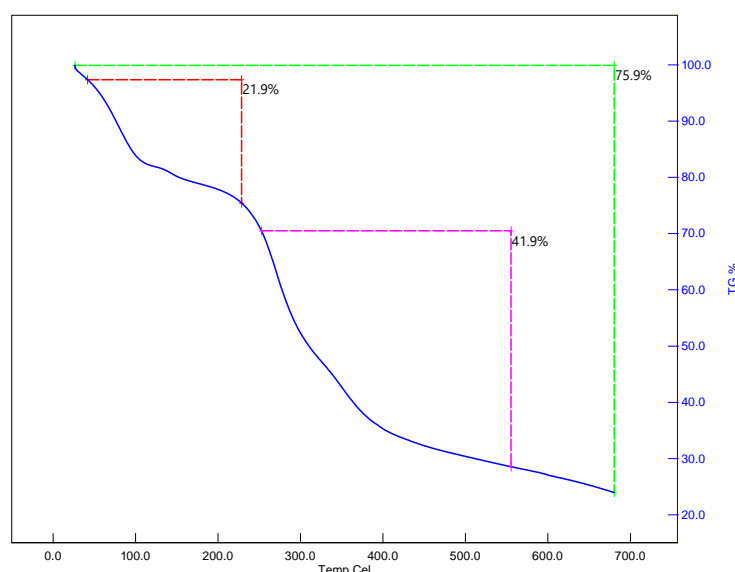


Figure 7. TGA graph of ZCP

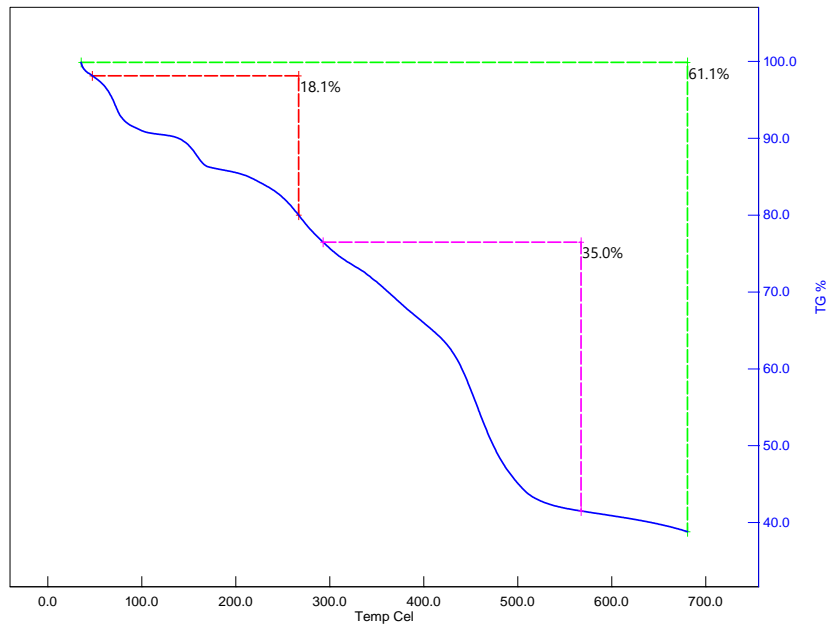


Figure 8. TGA graph of DCP

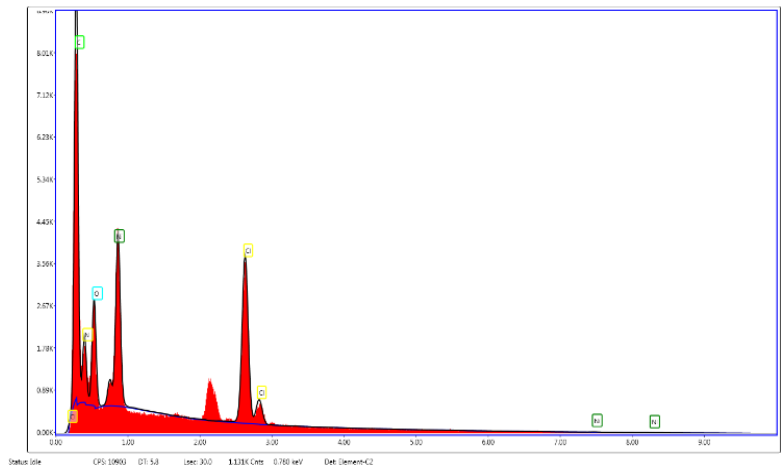
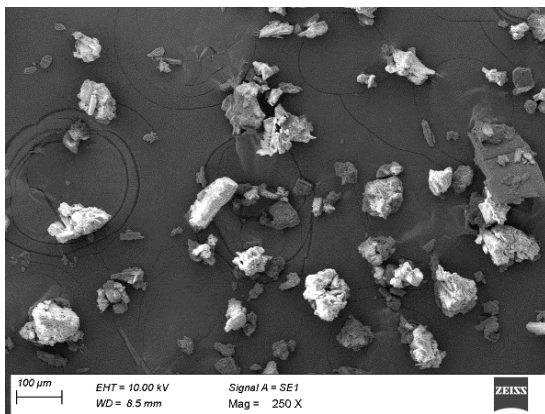


Figure 9. SEM and EDX images of NCP

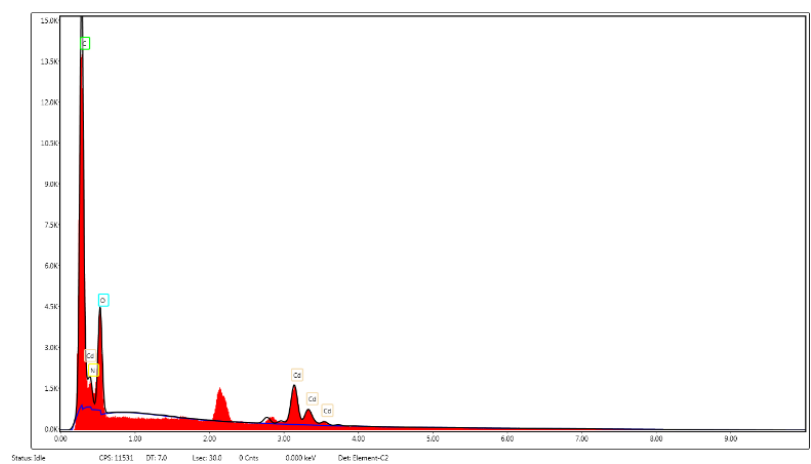
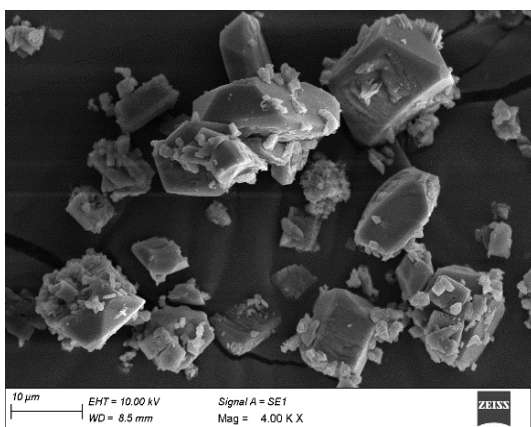


Figure 10. SEM and EDX images of DCP

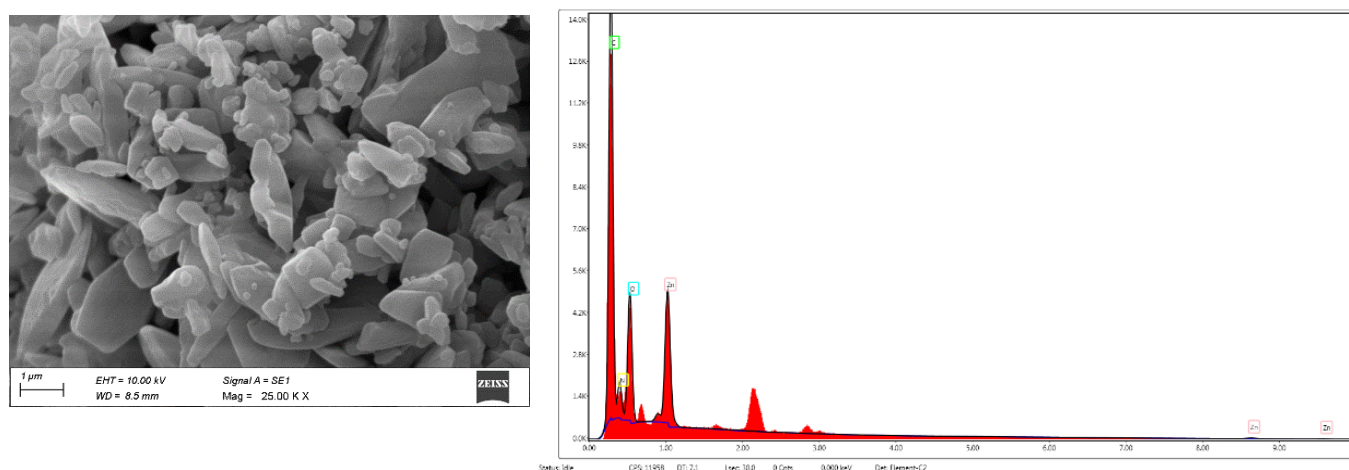


Figure 11. SEM and EDX images of ZCP

The cadmium complex displayed agglomerated, irregularly shaped particles, indicating strong interparticle interactions. The zinc complex exhibited a crystalline morphology with well-faceted particles, suggesting ordered molecular packing within the solid-state structure. The observed variations in surface morphology correlate well with the coordination environment of the metal centres and their interaction with the organic ligands [24-26]. The EDAX data depicted are also in accordance with the predicted structure.

4. Conclusion

The successful synthesis and detailed analysis of transition metal complexes with CHDA and Phen ligands revealed significant insights into their structural coordination, thermal behavior, and morphology. The distinct coordination patterns confirmed through FT-IR and PXRD analyses, along with the thermal stability profiles from TGA, highlight the robustness of these complexes. SEM imaging further supported the influence of metal centers on surface architecture. These findings not only validate the role of CHDA and Phen as effective ligands for constructing stable metal-organic frameworks but also pave the way for their application in areas requiring thermally resilient and structurally diverse materials. Future studies can expand upon this work by exploring their functional performance in catalytic or sensing environments.

References

- [1] A. Wang, P.B. Huang, P.P. Sun, F.N. Shi, B. Tian, J. Gao, Synthesis and crystal structure of a Mn-based coordination complex as precursor for the synthesis of Mn₂O₃, *Inorganica Chimica Acta*, 498, (2019) 119166-2. <https://doi.org/10.1016/j.ica.2019.119166>
- [2] V.F. Shul'gin, Y.V. Trush, O.V. Konnik, E.B. Rusanov, V.Y. Zub, V.V. Minin, Binuclear copper (II) complexes with acyldihydrzones of 1, 4-cyclohexanedicarboxylic acid, *Russian Journal of Inorganic Chemistry*, 56(5), (2011) 707-712. <https://doi.org/10.1134/S0036023611050226>
- [3] B.H.M. Hussein, G.M. Khairy, R.M. Kamel, Fluorescence sensing of phosdrin pesticide by the luminescent Eu (III)-and Tb (III)-bis (coumarin-3-carboxylic acid) probes, *Spectrochimica Acta Part A: Molecular and Biomolecular Spectroscopy*, 158, (2016) 34-42. <https://doi.org/10.1016/j.saa.2016.01.008>
- [4] X. Xiong, L. Zhou, W. Cao, J. Liang, Y. Wang, S. Hu, F. Yu, B. Li, Metal-organic frameworks based on halogen-bridged dinuclear-Cu-nodes as promising materials for high performance supercapacitor electrodes, *CrystEngComm*, 19(47), (2017) 7177-7184. <https://doi.org/10.1039/C7CE01840A>
- [5] B.B. Beyene, G.A. Wassie, Antibacterial activity of Cu (II) and Co (II) porphyrins: role of ligand modification, *BMC chemistry*, 14(1), (2020) 51. <https://doi.org/10.1186/s13065-020-00701-6>
- [6] C.C. Corrêa, F.M. Scaldini, F.C. Machado, C.B. Pinheiro, Study of the supramolecular interactions of carboxylic acids used as versatile ligands in coordination chemistry, *Journal of Structural Chemistry*, 57, (2016) 1235-1242. <https://doi.org/10.1134/S0022476616060251>
- [7] M. Zhou, L. Song, F. Niu, K. Shu, W. Chai, A square-pyramidal copper (II) complex with



- strong intramolecular hydrogen bonds: diaqua (N, N'-dimethylformamide-κO) bis [2-(diphenylphosphoryl) benzoato-κO] copper (II), *Crystal Structure Communications*, 69(5), (2013) 463-466. <https://doi.org/10.1107/S0108270113008317/bg3156sup1.cif>
- [8] A.K. Bharati, Somnath, P. Lama, K. A. Siddiqui, A novel mixed ligand Zn-coordination polymer: Synthesis, crystal structure, thermogravimetric analysis and photoluminescent properties, *Inorganica Chimica Acta*, 500, (2020) 119219. <https://doi.org/10.1016/j.ica.2019.119219>
- [9] H. Mutlu Gençkal, M. Erkisa, P. Alper, S. Sahin, E. Ulukaya, F. Ari, Mixed ligand complexes of Co (II), Ni (II) and Cu (II) with quercetin and diimine ligands: synthesis, characterization, anti-cancer and anti-oxidant activity, *JBIC Journal of Biological Inorganic Chemistry*, 25(1), (2020) 161-177. <https://doi.org/10.1007/s00775-019-01749-z>
- [10] P. Jaividhya, M. Ganeshpandian, R. Dhivya, M. A. Akbarsha, M. Palaniandavar, Fluorescent mixed ligand copper (II) complexes of anthracene-appended Schiff bases: studies on DNA binding, nuclease activity and cytotoxicity, *Dalton Transactions*, 44(26), (2015) 11997-12010. <https://doi.org/10.1039/C5DT00899A>
- [11] J. Hu, H. Wang, Q. Gao, H. Guo, Porous carbons prepared by using metal-organic framework as the precursor for supercapacitors, *Carbon*, 48(12), (2010) 3599-3606. <https://doi.org/10.1016/j.carbon.2010.06.008>
- [12] Y. Zhang, M. Schulz, M. Wächtler, M. Karnahl, B. Dietzek, Heteroleptic diimine-diphosphine Cu(I) complexes as an alternative towards noble-metal based photosensitizers: Design strategies, photophysical properties and perspective applications, *Coordination Chemistry Reviews*, 356, (2018) 127-146. <https://doi.org/10.1016/j.ccr.2017.10.016>
- [13] S. Yuan, J.S. Qin, C.T. Lollar, H.C. Zhou, Stable metal-organic frameworks with group 4 metals: status and trends, *ACS central science*, 4, (2018) 440-450. <https://doi.org/10.1021/acscentsci.8b00073>
- [14] A.M.A. Adam, T.A. Altalhi, S.M. El-Megharbel, H.A. Saad, M.S. Refat, Using a Modified Polyamidoamine Fluorescent Dendrimer for Capturing Environment Polluting Metal Ions Zn²⁺, Cd²⁺, and Hg²⁺: Synthesis and Characterizations, *Crystals*, 11(2), (2021) 92. <https://doi.org/10.3390/cryst11020092>
- [15] M. Iqbal, M. Sirajuddin, S. Ali, M. Sohail, M.N. Tahir, O-bridged and paddlewheel copper (II) carboxylates as potent DNA intercalator: Synthesis, physicochemical characterization, electrochemical and DNA binding studies as well as POM analyses, *Inorganica Chimica Acta*, 440, (2016) 129-138. <https://doi.org/10.1016/j.ica.2015.10.042>
- [16] S. Shanjitha, K. Suvaranna, D. Sudha, S. Jone Kirubavathy, Potential of a novel binuclear Ni (II) single crystal to act as a luminescent platform for sensing Cd²⁺ - Crystal structure, spectroscopic and sensing studies. *Inorganica Chimica Acta*, 553, (2023) 121541. <https://doi.org/10.1016/j.ica.2023.121541>
- [17] Z. Di Zhou, S. Q. Li, Y. Liu, B. Du, Y.Y. Shen, B.Y. Yu, C.C. Wang, Two bis-ligand-coordinated Zn(ii)-MOFs for luminescent sensing of ions, antibiotics and pesticides in aqueous solutions, *RSC Advancse*, 12, (2022) 7780-7788. <https://doi.org/10.1039/D2RA00376G>
- [18] H. Kabeer, S. Hanif, A. Arsalan, S. Asmat, H. Younus, M. Shakir, Structural-Dependent N,O-Donor Imine-Appended Cu(II)/Zn(II) Complexes: Synthesis, Spectral, and in Vitro Pharmacological Assessment, *ACS Omega*, 5, (2020) 1229-1245. <https://doi.org/10.1021/acsomega.9b03762>
- [19] P.K. Yaman, H. Erer, Novel Coordination Compounds Based on 2-Methylimidazole and 2,2'-dimethylglutarate Containing Ligands: Synthesis and Characterization, *Journal of the Turkish Chemical Society Section A: Chemistry*, 5, (2018) 953-962. <https://doi.org/10.18596/jotcsa.420361>
- [20] X. Zhang, N. Xing, F. Bai, L. Wan, H. Shan, Y. Hou, Y. Xing, Z. Shi, Multi-functional d10 metal-organic materials based on bis-pyrazole/pyridine ligands supported by a 2,6-di(3-pyrazolyl)pyridine with different spanning flexible dicarboxylate ligands: synthesis, structure, photoluminescent and catalytic properties, *Crystal Engineering Communications*, 15, (2013) 9135-9147. <https://doi.org/10.1039/C3CE41213J>



- [21] C. Fan, X. Zhang, N. Li, C. Xu, R. Wu, B. Zhu, G. Zhang, S. Bi, Y. Fan, Zn-MOFs based luminescent sensors for selective and highly sensitive detection of Fe³⁺ and tetracycline antibiotic, *Journal of Pharmaceutical and Biomedical Analysis*, 188, (2020) 113444. <https://doi.org/10.1016/j.jpba.2020.113444>
- [22] A. Bartyzel, Synthesis, thermal study and some properties of N₂O₄—donor Schiff base and its Mn(III), Co(II), Ni(II), Cu(II) and Zn(II) complexes, *Journal of Thermal Analysis and Calorimetry*, 127, (2017) 2133–2147. <https://doi.org/10.1007/s10973-016-5804-0>
- [23] U. Usha, S. Chandra, Synthesis and Characterisation of Co(II), Ni(II), Cu(II) and Zn(II) Complexes of Some Thiosemicarbazones, *Synthesis and Reactivity in Inorganic and Metal-Organic Chemistry*, 22, (1992) 929–940. <https://doi.org/10.1080/15533179208016602>
- [24] X.F. Liu, X.Q. Guo, R. Wang, Q C. Liu, Z.J. Li, S.Q. Zang, T.C. W. Mak, Manganese cluster-based MOF as efficient polysulfide-trapping platform for high-performance lithium–sulfur batteries, *Journal of Materials Chemistry A*, 7, (2019) 2838–2844. <https://doi.org/10.1039/C8TA09973A>
- [25] S. Shanjitha, K. Suvarna, J. Zothanzama, N.S. Kumar, D. Premnath, S.J. Kirubavathy, Crystallization of 1, 4-cyclohexanedicarboxylic acid bridged tetra nuclear Cu(II) complex containing N–N chelating ligand – crystal structure, antimicrobial, antioxidant, cytotoxicity and electrochemical studies. *Journal of the Iranian Chemical Society*, 19, (2022) 4747–4760. <https://doi.org/10.1007/s13738-022-02639-z>
- [26] M.B. Solomon, A. Rawal, J.M. Hook, S.M. Cohen, C.P. Kubiak, K.A. Jolliffe, D.M. D’Alessandro, Electroactive Co(iii) salen metal complexes and the electrophoretic deposition of their porous organic polymers onto glassy carbon, *RSC Advances*, 8, (2018) 24128–24142. <https://doi.org/10.1039/C8RA04385J>

About the License

© The Author 2025. The text of this article is open access and licensed under a Creative Commons Attribution 4.0 International License.

Does this article screened for similarity?

Yes

Conflict of interest

The Author declares that there is no conflict of interest anywhere.